



Universidad Autónoma  
de Madrid

**Biblos-e Archivo**  
Repositorio Institucional UAM

**Repositorio Institucional de la Universidad Autónoma de Madrid**

<https://repositorio.uam.es>

Esta es la **versión de autor** del artículo publicado en:  
This is an **author produced version** of a paper published in:

Energy 174 (2019), 169-183

**DOI:** <https://doi.org/10.1016/j.energy.2019.02.158>

**Copyright:** © 2019 Elsevier

El acceso a la versión del editor puede requerir la suscripción del recurso

Access to the published version may require subscription

# TIME OF DAY EFFECTS OF TEMPERATURE AND DAYLIGHT ON SHORT TERM ELECTRICITY LOAD

Julián Moral-Carcedo <sup>(1)</sup>

Universidad Autónoma de Madrid

Julián Pérez-García

Universidad Autónoma de Madrid

## Abstract

This paper proposes a model for short-term electricity load with differentiated temperature and daylight effects by time of day, which are determined by variations in intraday economic activity. The relationship between electricity load and economic activity implies that the electricity demand response to changes in exogenous variables like temperature is non-linear as well as non-homogeneous along the day. The proposed framework, a smooth transition regression model with double threshold (LSTR2), models the observed intraday patterns in load curves to explicitly capture the effect of the circadian rest-activity cycle on the distinct responses of electricity demand to temperature and daylight variations throughout the day. The model shows that the sensitivity of demand to low temperatures is significantly larger in the “active” compared to the “rest” state. If temperatures decrease from 10 °C to 0 °C, electricity demand in the “active” state increases by 960.5 MWh per 1°C decrease, but by only 26.6 MWh per 1° C decrease in the “rest” state. When temperatures are higher, in the “rest

---

<sup>1</sup> Corresponding author. (\*) E-mail: julian.moral@uam.es Universidad Autónoma de Madrid. Fac. CC. Económicas. Campus de Cantoblanco. Madrid 28049. Spain.

(\*\*) E-mail: julian.perez@uam.es Universidad Autónoma de Madrid. Fac. CC. Económicas. Campus de Cantoblanco. Madrid 28049. Spain.

state” demand decreases by 602.9 MWh per 1° C if temperature falls from 26°C to 21°C, while in the “active” state demand only decreases by 323.6 MWh per 1°C variation.

*JEL classification:* Q4, L94, C53

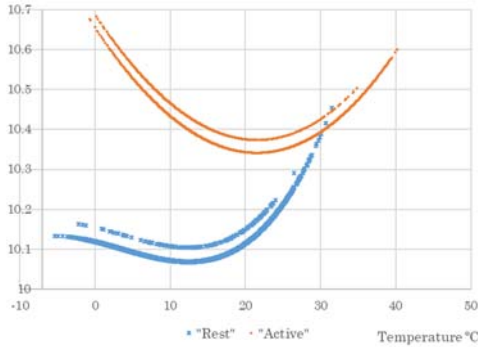
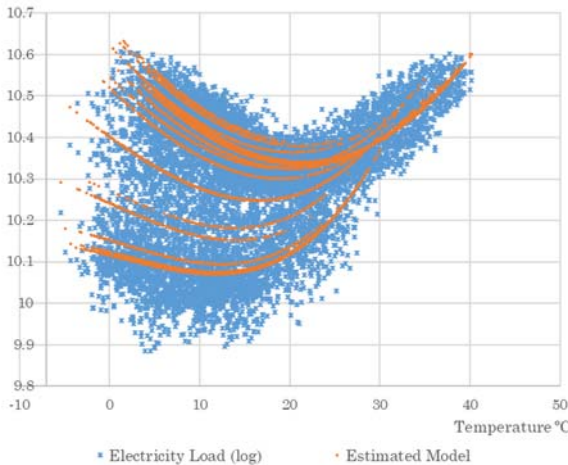
*Keywords:* short-term electricity load, temperature effect, daylight effect, circadian cycle.

## Highlights

1. Load data shows that the temperature effect is both non-linear and non-homogenous.
2. Time properties of economic activity directly translate into the shape of load curves.
3. Economic activity also affects the way temperature influences the electricity load.
4. A model for hourly electricity load with differentiated temperature effects by time of day is proposed.
5. The proposed model captures well the higher sensitivity of electricity demand to temperatures in the “active” state.

# Graphical Abstract

Hourly electricity load (MWh logs) and temperature. Estimated electricity demand response for the “rest” and “active” state of economic activity.



# 1. INTRODUCTION

Electricity is a key input for productive activities, and hence economic activity strongly determines electricity demand. This relationship holds true at different time horizons. In the long run, the relationship is reflected in the link between economic growth and electricity consumption, while in the short run, electricity demand is very sensitive to the weekly cycle of economic activity induced by the succession of workdays and weekends as well as holidays, see e.g. [1], [2], [3], [4] among others.

Moreover, in the very short run the intraday cyclical nature of economic activity, which in the end is related to the circadian rest-activity cycle, is also reflected in electricity demand. Working time, opening hours, school schedules, leisure time, etc. shape electricity loads throughout the day and throughout the week.

In Spain, the peak of hourly electricity demand in the winter occurs on cold days just after sunset (19h-20h), see e.g. [5.], or [6.] and [7.]. In the summer, hourly electricity demand is highest on hot days around 13-14h. However, surprisingly, these are not the hottest hours of the day (see Figure A-1 in the Appendix). This reveals the key role of the daily rest-activity cycle for understanding the factors behind the shape of the electricity load curve and how the effect of temperature on demand is altered by business activity cycle. Given the prospect of global warming, the analysis of how and when changes in outside temperatures affect electricity demand is particularly important. Furthermore, the mix of generation technologies also changes throughout the day. Usually during hours of peak demand, generation of electricity involves technologies that emit more carbon dioxide such as coal, gas or fuel power plants. Therefore, analyzing how electricity demand reacts

to changes in temperatures and daylight, depending on time of day, is not only relevant for estimating electricity demand correctly. It is also a first step towards a better understanding of how demand response policies can contribute to mitigate carbon emissions.

In this paper, the observed intraday patterns in load curves are modelled to explicitly capture the effect of the circadian rest-activity cycle on the distinct responses of electricity demand to temperature and daylight variations throughout the day. Existing models in the literature typically include temperature variables to model electricity load. However, they usually do not include daylight duration explicitly. To deal with the rest-activity cycle, electricity load is usually modelled for each hour separately as in [5.], [8.], [9.], and [10.]. Other approaches approximate daily activity cycles by cyclical “footprints,” including lagged electricity loads as explanatory variables and applying ARIMA, SARIMA, or exponential smoothing models [2.], [13.], and [14.]. There also exist models that attempt to identify electricity load profiles by repeated application of clustering techniques, artificial neural networks, or restricted Boltzmann machines (see e.g. [11.], [12.], [15.], or [16.]) . However, to the best of our knowledge, the proposed model is the first to explicitly capture the rest-activity cycle and its interaction with temperature and daylight duration to explain short-term electricity demand. In particular, a novel and simple procedure is proposed using well-known modelling techniques based on underlying “hidden states”. Comparing the results from the model that employs a Logistic Smooth Switching Regression controlled by a double threshold (LSTR2) to results from the well-known Hidden Markov Model (HMM), it can be concluded that the first model fits the features of the data better.

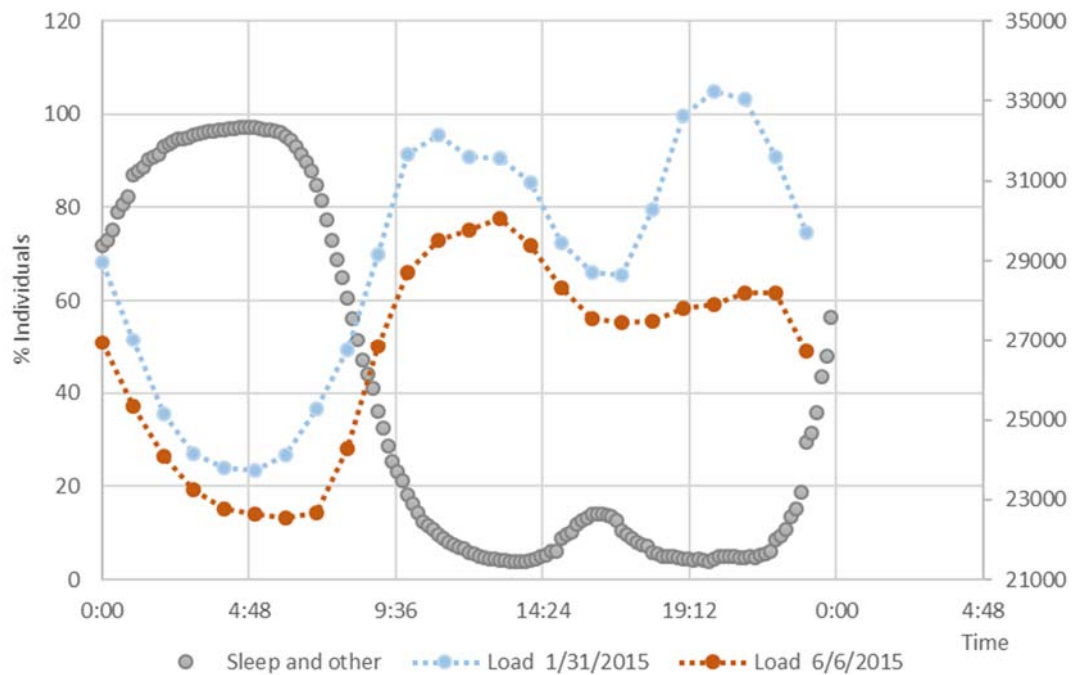
The remainder of this paper is organized as follows. The next two sections describe the data and the different cycles in hourly electricity load curves.

Section 4 analyses the temperature effect on electricity demand using hourly data, and highlights why it is necessary to take into account the daily rest-activity cycle to adequately interpret the observed responses of electricity load to temperature changes. Section 5 presents the modelling approach. Section 6 compares our results to the ones obtained from using the state-of-the-art HMM methodology, and finally Section 7 concludes.

## 2. CYCLICAL PATTERNS IN ELECTRICITY LOAD

On a typical workday (see Figure 1), electricity demand in Spain registers very high levels between 7h and 16h, which is the typical working time in industrial, commercial, and public sector activities. We also observe relatively high levels of electricity demand between 16h and 23h due to residential demand of households and demand by retail and commercial sectors with opening hours until 20-21h. The lowest values for electricity consumption are recorded between 23h until 6h the following day, with an absolute minimum around 3-4h. This obviously coincides with the usual hours of sleep in Spain. On holidays and Sundays, hours of highest electricity consumption differ slightly and lie between 9-23h, while the absolute minimum is recorded between 4-6h.

Figure 1 Participation rate in the activity “Sleep and other personal care” (left y-axis; % individuals) and electricity load curves in winter (31/01/2015) and spring (6/6/2015) for Spain (right y-axis; MWh)



Sources: Harmonized European Time Use Survey for the share of individuals sleeping and REE S.A. for electricity load curves.

Independently of the particular time of year, in Figure 1 a clear inverse relationship between the fractions of individuals participating in the activity “Sleep and other personal care” and electricity demand can be observed. This is not surprising given that electricity is a variable input to production, and hence when most individuals are sleeping and fewer economic activities are



being carried out, lower consumption of electricity is observed.<sup>2</sup> Furthermore, the level of electricity consumption also depends on the installed equipment (lighting, air conditioning, home appliances, etc.). For a given level of energy efficiency, increased penetration of appliances entails higher electricity consumption, but again only during hours when these appliances are being used. For instance, in the case of air conditioning equipment, electricity consumption depends on outside temperatures and thermal inertias that determine how comfort and inside temperatures differ. However, electricity consumption also depends on the degree of penetration of such equipment in households and in the commercial sector. Moreover, variations in economic activity throughout the day determine the use of air conditioning equipment and hence the degree to which temperature increases lead to higher electricity consumption. Therefore, depending on the time of year and even on the time of day, different responses in electricity load curves to variations in outside temperature will be observed, regardless of the particular variation in temperature throughout the day. In Section 3, the relationship between hour of day and temperature will be analyzed in detail. In particular, it will become clear how intraday economic activity alters the response of electricity demand to temperature variations.

However, not only outside temperatures<sup>3</sup> drive electricity loads in the very short run. Daylight duration also has a remarkable and variable effect on

---

<sup>2</sup> For industrial activities that use electricity as their main energy source and as a direct input for production, the higher the output, the higher the level of electricity consumption. However, in commercial and service sector activities this link is weaker because electricity is used as an indirect input for cooling, heating, and lighting. For instance, for a shopping mall located in a hot climate zone, electricity consumption depends more on temperature variations than on sales.

<sup>3</sup> It is important to note that outside temperatures are also directly affected by daylight. Therefore, it could be argued that the observed patterns in electricity load curves are completely due to temperature variations. It is true that when temperatures are high (low), higher (lower) temperatures shift the load curve upwards. However, the intraday profile of the electricity load curve is much smoother around the hours of sunset and sunrise compared to the profile of temperatures. Moreover, the observed declining electricity load in the afternoon until sunset, both in winter and

electricity demand. Similar to the case of temperature, more equipment for lighting implies higher levels of electricity consumption, but again only during certain hours. In particular, demand for lighting is clearly observed after sunset, but only for a limited period of time, as most lights are switched off during periods of sleep at homes and closing hours of businesses. As daylight duration varies depending on the time of year, electricity consumption linked to lighting differs throughout the year and even across regions. Spain's geographical coordinates (latitude and longitude) are such that throughout the year the sun rises between 6.40h and 8.38h while sunsets occur between 17.48h and 21.49h. Hence, depending on the time of year, daily economic activity in Spain sometimes needs to employ artificial light.

The effect of the variability in daylight duration on electricity demand can be observed in Figure 2 where two electricity load curves for Spain on a typical day in winter (February 16<sup>th</sup>) and summer (July 22<sup>nd</sup>) are displayed. Figure 2 also shows electricity load curves for Singapore on these same days. Singapore is located on the latitude 1° 17' 24.9720" N, and hence very close to the equator, leading to a very similar duration of daylight throughout the year. Spain's latitude coordinates are 40° 25' 0" N (Madrid), which implies that daylight duration is much longer in the summer than in the winter.<sup>4</sup> As a result, while electricity load curves for Singapore display a very similar

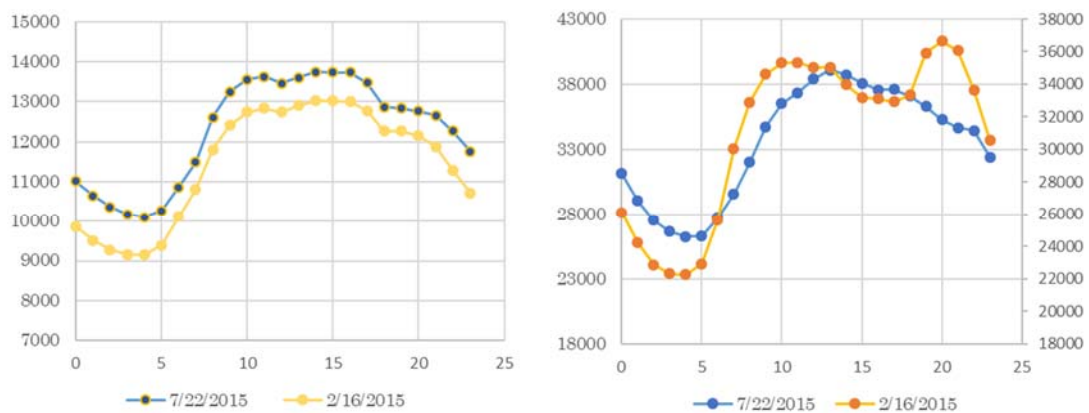
---

summer, occurs when temperatures are still increasing in summer and decreasing in winter. Therefore, observed changes in the shape of electricity load curves throughout the year cannot be completely explained by variations in temperature (see Figure A-1 in the Appendix for hourly temperatures in Spain on typical days in winter and summer).

<sup>4</sup> For instance, on a typical day in winter (Feb 16<sup>th</sup> 2015) hours of sunrise and sunset were 8:08 and 18:51 in Spain and 7:17 and 19:21 in Singapore, compared to 7:03 and 21:39 in Spain and 7:06 and 19:17 in Singapore on a typical summer day (July 22<sup>nd</sup> 2015) - National Oceanic & Atmospheric Administration (NOAA) calculator-<http://www.esrl.noaa.gov/gmd/grad/solcalc/>.

shape in summer and winter, in Spain there are marked differences, especially around the hours of sunrise (7-8h) and sunset (19-21h).

*Figure 2.-Electricity load curves (MWh) for Singapore (left) and Spain (right) on a typical day in winter (16/2/2015) and summer (22/7/2015).*



Source: Singapore Energy Market Authority, Spain REE S.A.

Seasonal variations in temperatures and daily temperature amplitude (difference between the minimum and maximum temperature on a given day) are intimately related to seasonal changes in daylight duration. However, each factor implies different uses of electricity and different time patterns of electricity use. Hence, to understand short-term electricity loads, temperature and daylight effects on electricity demand need to be analyzed separately and together with the daily rest-activity cycle.

### 3. DATA AND DESCRIPTIVE ANALYSIS

The data on hourly electricity loads come from the Spanish system operator, Red Eléctrica de España (hereafter, REE). In particular, in this paper data for the period 01/01/2015 to 31/12/2016 is considered, and hence our sample consists of 17,544 hourly observations. Between 2015 and 2016 annual electricity demand in Spain remained almost constant, increasing by only 0,7%. This is important because the modelling approach proposed assumes that long-term drivers of electricity demand such as population growth or growth in investment in equipment remain constant, something that seems to be fulfilled for this time period.

The left-hand graph of Figure 3 displays the continuous wavelet transform (CWT) of our hourly electricity load data. The relationship between the hourly electricity load and the timing (hours) of economic activity induces easily identifiable characteristics into the magnitude scalogram. The daily activity cycle between 7h and 23h induces a marked cyclical component every 24 hours into electricity demand; i.e. at a frequency of  $1/24=0.04167$  per hour. For comparison, the second graph of Figure 3 displays the continuous wavelet transform (CWT) of simulated daily cycles with the frequency concentrated at exactly 0.04167 (the underlying data are depicted in the second graph of Figure 4). Furthermore, as clearly visible in the wavelet transform of our data, the weekly succession of workdays and weekends also induces a weekly component every 7 days (168 hours) into electricity demand; i.e. at a frequency of  $1 / (24*7)= 0.00595$  per hour. Again, for comparison the third graph of Figure 3 is displayed a continuous wavelet transform (CWT) of simulated weekly cycles with the frequency concentrated at exactly 0.00595. Finally, national holidays as well as holiday

periods (in the summer and during Christmas time) induce less marked seasonal characteristics into electricity demand. These are concentrated at lower frequencies [0 - 3 10<sup>-6</sup>]. However, they are not identifiable at a mere glance due to the role of other seasonal factors, mainly the variation in temperatures throughout the year, closely linked to changes in daylight duration (see Figure 5).

Figure 3.-Continuous 1-D wavelet transform of hourly electricity load data and comparison with simulated patterns for Spain. (17,544 hourly obs.).

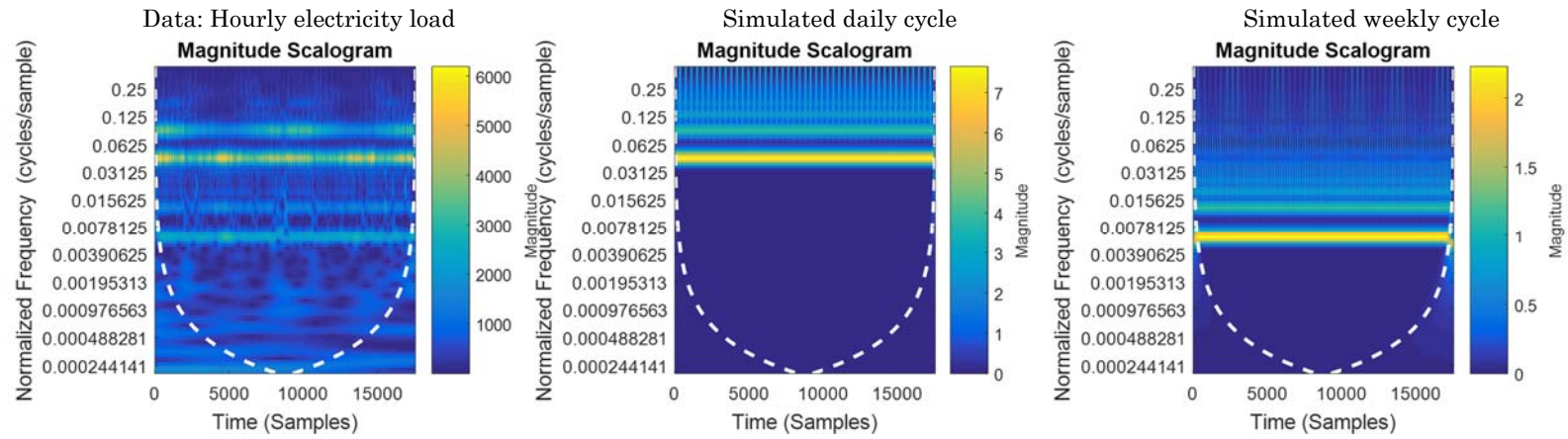


Figure 4.- Hourly electricity load data for Spain for January 2015, and examples of daily ( period of 24h.) and weekly cycles (period of 24 x 7 h.) . (336 hourly obs.).

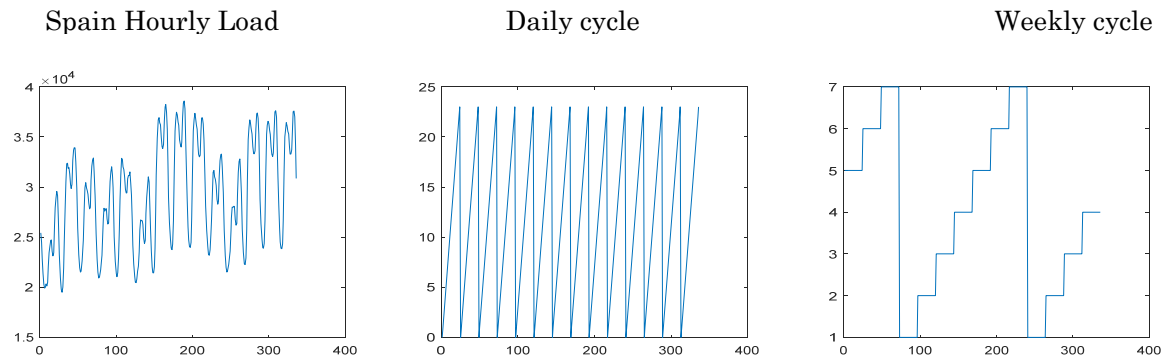
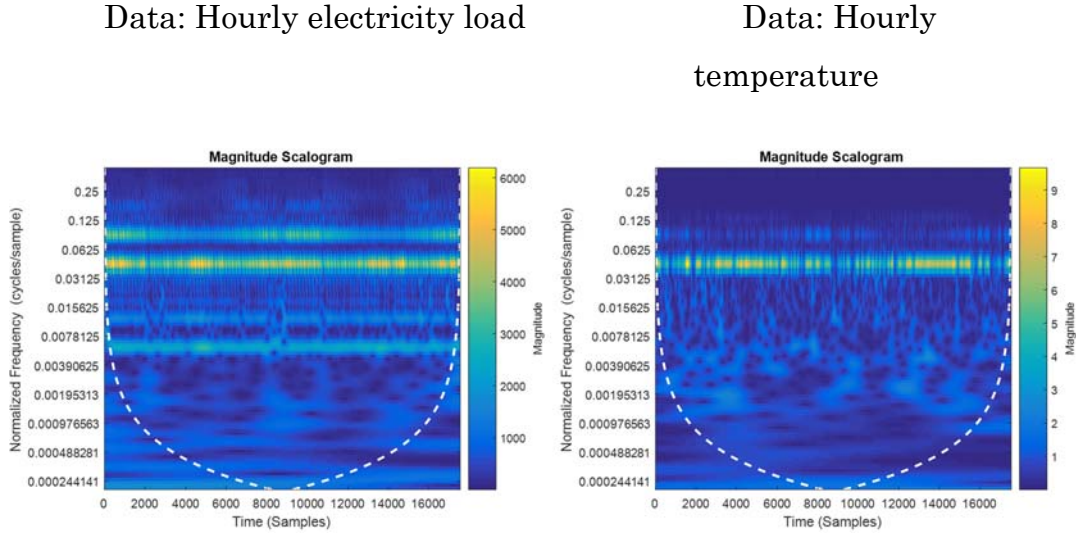


Figure 5.-Continuous 1-D wavelet transform of hourly electricity load data and hourly temperature data for Spain, 2015-2016. 17,544 hourly obs.



One simple and intuitive way to highlight how seasonal factors which are partially hidden by the dominant 24-hour cycle affect electricity load, is to analyze load data for each hour as in [8.], [9.], [10.] or [5.]. Another interesting possibility, explored below, is to apply load curve clustering, i.e. analyzing clusters of daily profiles of hourly electricity loads, where  $\mathbf{d}_t = [d_t^0, d_t^1, \dots, d_t^{23}]$  is the 24-hour vector of observed electricity consumption on a given day. This procedure preserves the full shape of the load curve on a given day, making it possible to identify different shapes of load curves throughout the year. In particular, different shapes of load curves are associated to certain types of days and allow us to identify seasonal factors other than intraday variations, which affect electricity demand. For this analysis, daily load curves are grouped into clusters, or seasonal profiles,

using a  $k$  means clustering procedure with eight types of days<sup>5</sup> and using the square Euclidian distance.

Figure 6 displays the result of load curve clustering applied to our data for 2015. The identified clusters or profiles are displayed in a “calendar” plot next to the 24-hour load profiles of the centroids. This representation allows to immediately see the dates of seasonal patterns identified by the clusters. Three main features become apparent. First, weekends and national holidays (January 1<sup>st</sup> and 6<sup>th</sup>, March 19<sup>th</sup>, April 2<sup>nd</sup> and 3<sup>rd</sup>, May 1<sup>st</sup>, October 12<sup>th</sup> and December 8<sup>th</sup> and 25<sup>th</sup>) always belong to clusters which are different from those of adjacent workdays. Second, August when the vast majority of Spaniards are on holiday is a very atypical month, which is reflected in the high number of different load profiles. Third and more interesting, a clear seasonal pattern in load curves is observed that can be directly related to the four seasons and the solstices in winter and summer as well as the equinoxes in spring and autumn. This seasonal pattern in electricity demand is related to both the temperature effect and daylight duration. Regarding the former, some of the clusters clearly reflect the role of temperature for electricity demand. For instance, cluster 2 is composed of hourly load data observed on workdays in July 2015, one of the hottest months registered in Spain. Cluster 6 on the other hand is composed of electricity loads observed on some of the coolest workdays in winter (January and February). To highlight the effect of daylight duration on electricity demand, peak loads in the afternoon across different clusters are considered. In particular, the effect becomes evident when comparing load curves of cluster 5 (workdays in November and December) where the peak is located at 19h and cluster 2 (workdays in July) where it is located at 21h.

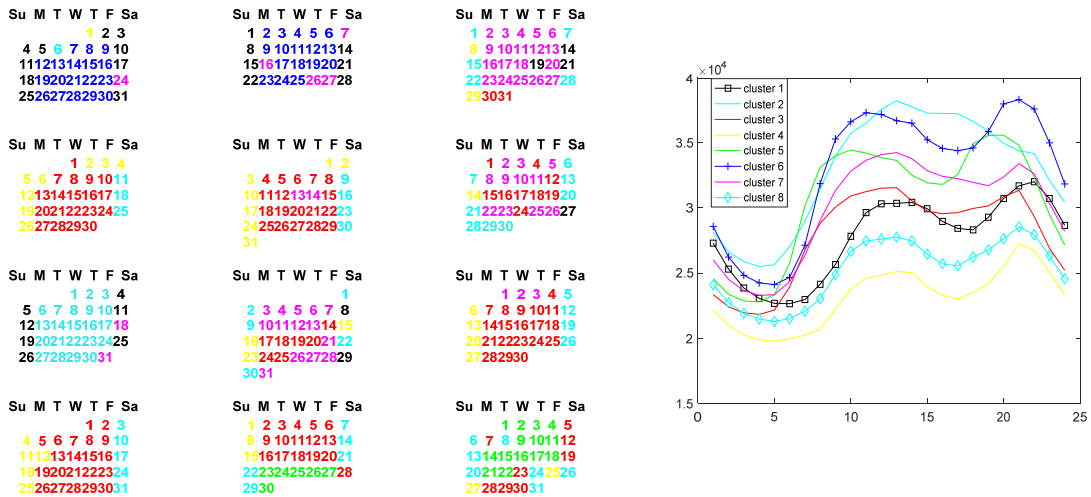
---

<sup>5</sup> The number of groups has been determined by an iterative procedure, starting with one group and increasing the number of groups until the sum of within-cluster sums of point-to-centroid distances in two consecutive iterations increases.



The reported interaction between the temperature effect and daylight duration and their effect on the seasonal pattern in electricity demand highlight why it is necessary to include several seasonal (weekly and monthly) dummy variables if electricity load is analyzed hour by hour. In Section 4, a different approach is proposed that enables us to analyze the full load curve instead of analyzing it hour by hour.

Figure 6.- Calendar plot of load profiles (left) and load profile of centroids (right) obtained applying load curve clustering to hourly electricity load data for Spain for 2015.



Note: From Left to Right: January, February, etc.

## 4. TEMPERATURE EFFECT

Temperature is a key driver of electricity demand; see e.g. [17.], [1.], [18.], [19.], [20.], [21.], [22.], or [23.] among many others. In particular, temperature has a direct impact on aggregate electricity consumption because of the need to adjust inside temperatures whenever they deviate from comfort temperatures due to variations in outside temperature. Electric appliances and uses of electricity are essentially climate and region-specific. In countries like Spain with extreme winters and summers, temperature affects electricity demand in a nonlinear fashion because of different energy usage patterns whenever temperatures are low (demand for heating) or high (demand for cooling). When temperatures are low as during the winter, increasing temperatures have a negative effect on electricity demand, and hence demand decreases with higher temperatures. If on the other hand temperatures are high as during the summer, electricity demand and temperatures move in the same direction. Hence, we observe a u-shaped relationship between temperature and electricity demand.

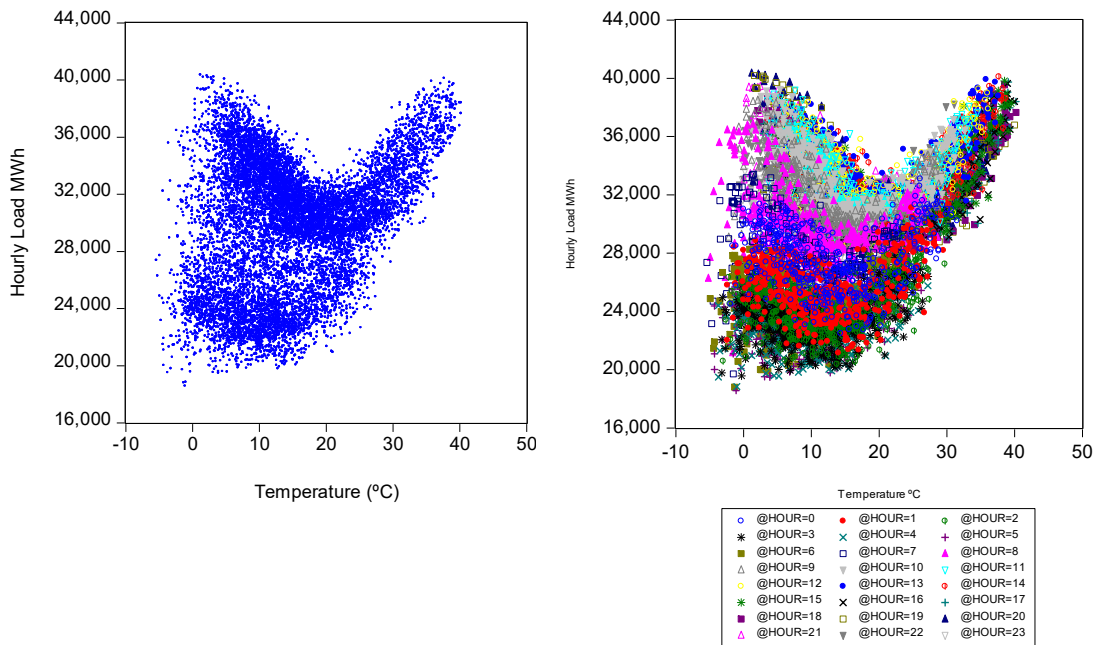
The left-hand graph of Figure 7 displays hourly electricity load data for 2015 and 2016<sup>6</sup> (workdays only, and excluding August) against temperatures. At first glance, it is difficult to observe the expected u-shaped relationship between temperature and electricity demand. However, this changes when data are differentiated by hour of day, as in the right-hand graph of Figure 7. Here we observe a u-shaped relationship between temperature and electricity demand. However, it also becomes clear that the exact relationship changes with each hour, suggesting that the approach followed

---

<sup>6</sup> For this relatively short period (2 years), we assume that growth in long term factors (GDP, population, equipment, etc.) and changes in efficiency affecting electricity demand can be neglected.

by [8.], [9.], [10.] or [5.] where load data is analyzed for each hour separately could be more appropriate

Figure 7.- Hourly electricity load and temperatures (2015-2016)



Note: Data for holidays, weekends, and the month of August are excluded.

However, modelling the temperature effect hour by hour may lead to results that are difficult to interpret. Assume that  $E_t^i$ , electricity load (in logs) of hour  $i$  on day  $t$  depends nonlinearly on temperature, following an unknown function like,

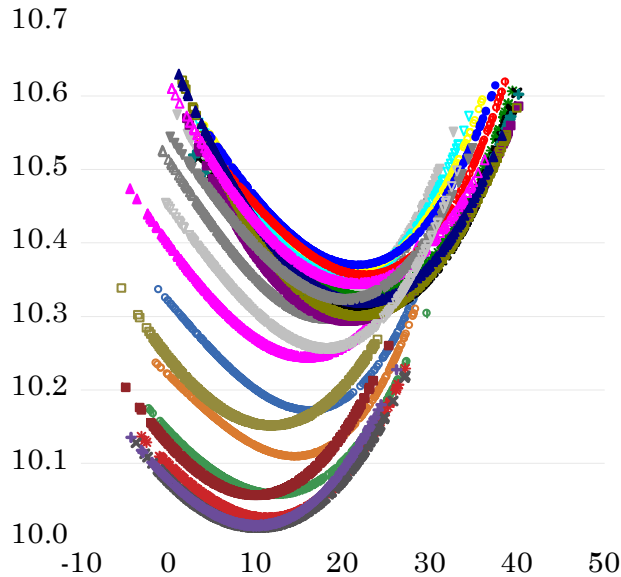
$$E_t^i = f(T_t^i); i=0,1,\dots,23 .$$

The function  $f(T_t^i)$  can then be estimated by a third-order polynomial expansion in  $T_t^i$ , as follows

$$E_t^i = f(T_t^i) = a_0^i + a_1^i T_t^i + a_2^i T_t^{i2} + a_3^i T_t^{i3} + \epsilon_t^i.$$

After estimating parameters  $\{a_j^i, i = 0,1,..23 ; j = 0,1,..3\}$  by ordinary least squares, it is possible to obtain the hourly estimated temperature responses<sup>7</sup> plotted in Figure 8. Although the expected u-shaped relationship between temperature and electricity demand can be observed, the temperature effect is non-homogenous across hours. In particular, between 3h and 20h the u-shaped relationship seems to shift upwards and to the right, while we observe a downright and leftward shift between 21h and 2h.

Figure 8 Hourly electricity load (MWh logs) and temperatures (°C). 2015-2016



Note: Data for holidays, weekends, and the month of August are excluded

<sup>7</sup> Estimation results are included in the Appendix.

This shift of the temperature-electricity curve does not only affect the theoretical threshold of demand response changes to temperatures (in the literature an outdoor temperature threshold of 19-20°C is commonly found). It also alters the gradient of the load response of electricity demand to temperature changes, i.e. the increase in electricity demand as temperature changes by 1°C. In particular, between 2h and 6h the u-shaped curve is much flatter, and the threshold demand response lies between 10-15°C. Over the following hours of the day, the u-shaped curve becomes much steeper and the temperature threshold moves from 12°C (at 7 h) to 22°C (at 15 h). The change in the temperature threshold throughout the day can be explained by the effect of thermal inertias on indoor temperatures, which are the true drivers of electricity demand whenever they differ from comfort temperature. The change in the elasticity of the demand response, however, reflects the relevance of other variables which affect the intraday electricity load pattern. This paper follows the hypothesis that the level of economic activity changes the observed response of electricity demand to temperatures. In particular, we expect is that the way temperature affects electricity demand will not be the same under full business and household activity during the day, than with very low economic activity during the night. The next section details the proposed model that is able to explain variations in short-term electricity load by incorporating how economic activity interacts with temperature and daylight effects.

## 5. MODELLING STRATEGY

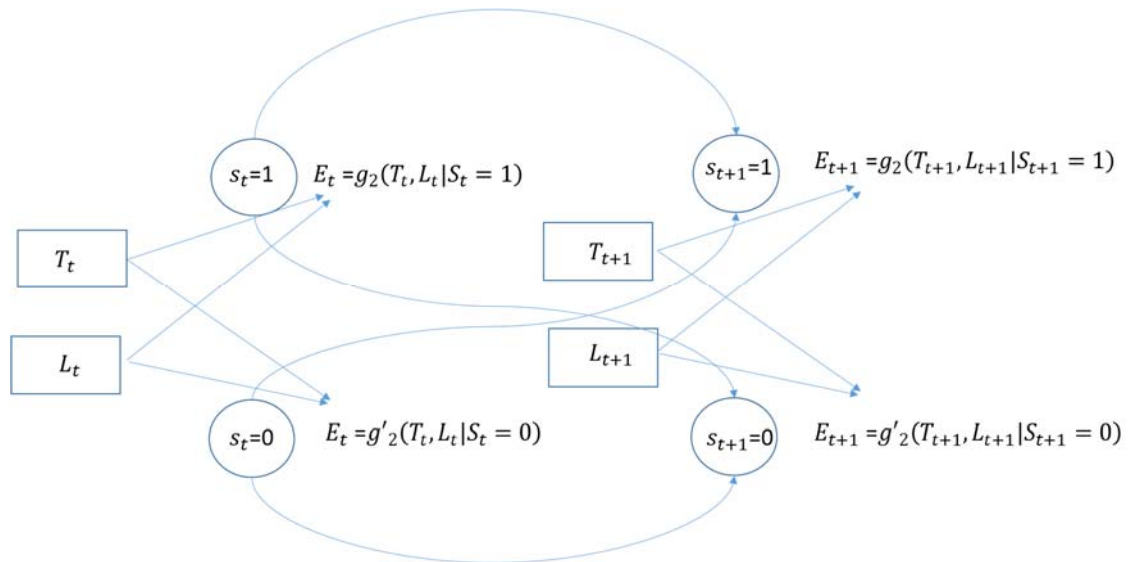
Hourly electricity load can be modeled as the interaction between several effects, such as hour of the day, temperature, type of day, daylight duration, as well as a factor  $s$  affecting electricity demand in the long run. We define  $E_t$  as the hourly electricity load (in logs) observed at time  $t$ , which is defined by an hour  $h$  ( $h=0,1,2,..23$ ) and a type of day  $W_d$ , and we assume that the different effects interact (see Figure 9) according to:

$$E_t = f(h, W_d, T_t, L_t, O_t) = g_1(h, W_d)g_2(T_t, L_t)g_3(O_t) \quad [\text{Eq. 1}],$$

where  $T_t$  is the temperature in °C observed at time  $t$ ,  $L_t$  denotes lighting needs determined by daylight duration, and  $O_t$  are other, low frequency events which affect electricity load (economic activity, population growth, etc.). The functions  $g_i$  (where  $i = 1,2,3$ ) capture how each effect influences electricity load.

In order to make the model tractable the following assumptions are imposed. First, it is assumed that during relatively short periods of time (e.g. less than 2 years) other variables  $O_t$  remain constant, and hence their effect on electricity load variations can be neglected. For longer time periods, the effect of  $O_t$  could be captured by a simple trend term given that the underlying variables tend to evolve rather smoothly. Second, for simplicity only two types of days are considered: workdays (excluding August) and other days (weekends and holidays). For a given hour  $h=0,1,2,..,23$  of a day type  $W_d$ , the function  $g_1(h, W_d)$  maps each hour of the day into a real value belonging to the  $[0,1]$  interval, i.e.  $s_t = g_1(h, W_d)$ , where  $s_t \in [0,1]$ .

Figure 9.- *Modelling the effect of temperature ( $T_t$ ) and lighting needs ( $L_t$ ) on electricity load depending on the unobserved state of “economic activity.”*



The function  $s_t = g_1(h, W_d)$  can be interpreted as a function for the probability of being in a hidden “active state” of economic activity. If  $s_t = 0$ , then economic activity is in a “rest” state, and if  $s_t = 1$  economic activity is in an “active” state. If for hour  $h$  the function  $g_1(h, W_d)$  takes on a value of 0, economic activity at this hour is very low and other drivers of electricity consumption (lighting needs, cooling and heating needs, etc.) will only have a reduced impact on aggregate electricity consumption. At the other extreme, if for hour  $h'$  the function  $g_1(h', W_d)$  takes on a value of 1, then there is full economic activity at this hour and other drivers will have a large impact on aggregate electricity consumption. Given that economic activity throughout the day is not expected to behave as a “jump” process, but rather

that it transitions smoothly between states,  $g_1(h, W_d)$  is assumed to be a smooth transition function. In particular,  $g_1(h', W_d)$  is assumed to be a quadratic logistic function with double threshold (LSTR2)

$$g_1(h', W_d, \gamma_d, \tau_1, \tau_2) = \frac{1}{1 + \exp[-\gamma_d(h - \tau_1)(h - \tau_2)]}, \quad [\text{Eq. 2}]$$

where  $\tau_1$  and  $\tau_2$  are parameters for the threshold hours indicating when the “active” state of economic activity starts and ends respectively. Parameter  $\gamma_d$  modulates the speed of transition between the “rest” and “active” states, and as such allow characterizing how transitions between states occur.

In Equation [1], the effect of temperatures and daylight duration is captured by the term  $g_2(T_t, L_t)$ , assumed to be a nonlinear function. However, to avoid additional complexity it is assumed that this function is additively separable in its arguments,  $g_2(T_t, L_t) = g'_2(T_t) + g'_2(L_t)$ . The function  $g'_2(T_t)$  will be linearized by polynomial expansions of degree 3 in  $T_t$ , and  $g'_2(L_t)$  will be linearized in  $L_t$ , which is a binary variable that takes on value 1 if  $t$  belongs to the period between sunset and sunrise (night), and 0 otherwise.<sup>8</sup> The interaction between  $g_2(T_t, L_t)$  and the activity effect  $g_1(h, W_d)$  implies that temperature and lighting needs will have different effects on electricity demand if economic activity is in an “active” or in a “rest” state. In particular, if at time  $t$  economic activity is in a “rest” state ( $s_t = 0$ ), then electricity load will be determined by model  $g_2(T_t, L_t)$ . If on the other hand, economic activity is in an “active” state ( $s_t = 1$ ), then electricity load will be determined by model  $g'_2(T_t, L_t)$ . Put differently,  $g_1(h, W_d)$  can be interpreted

---

<sup>8</sup> Data on times of sunset and sunrise are obtained from the NOAA calculator (National Oceanic & Atmospheric Administration). Temperature data is from Ru5



as the probability of being in each state, and the expected electricity load at time  $t$ ,  $E[E_t]$ , is then given by

$$E[E_t] = g_1(h, W_d)g_2(T_t, L_t) = g_2(T_t, L_t)[1 - g_1(h', W_d, \gamma_d, \tau_1, \tau_2)] + g'_2(T_t, L_t)g_1(h', W_d, \gamma_d, \tau_1, \tau_2), \quad [\text{Eq. 3}]$$

where  $g_1(h', W_d, \gamma_d, \tau_1, \tau_2) = \frac{1}{1 + \exp([- \gamma_d(h - \tau_1)((h - \tau_2))])}$  is the unconditional probability of being in an “active” state ( $s_t = 1$ ). Note that this probability is fully determined by  $h$ , once parameters  $\gamma_d$ ,  $\tau_1$ , and  $\tau_2$  have been estimated.

A convenient specification of the model, introducing the linearity assumption regarding  $g_2(T_t, L_t)$ , is the following,

$$E_t = g_1(h, W_d, \gamma_d, \tau_1, \tau_2)g_2(T_t, L_t) = [\beta_o + \beta_1 T_t + \beta_2 T_t^2 + \beta_3 T_t^3 + \beta_4 L_t] + [\beta'_o + \beta'_1 T_t + \beta'_2 T_t^2 + \beta'_3 T_t^3 + \beta'_4 L_t]g_1(h', W_d, \gamma_d, \tau_1, \tau_2) + \varepsilon_t, \quad [\text{Eq. 4}]$$

where  $\varepsilon_t$  captures approximation errors to the unknown function  $g_2(T_t, L_t)$ . These errors are expected to exhibit some degree of correlation of a similar order as the dominant periodicity in variables  $T_t$  and  $L_t$ .

Alternatively, Eq 4 can be expressed as

$$E_t = \begin{cases} \beta_o + \beta_1 T_t + \beta_2 T_t^2 + \beta_3 T_t^3 + \beta_4 L_t + \varepsilon_t & ; \text{ if } g_1(h, W_d) = 0 \\ (\beta_o + \beta'_o) + (\beta_1 + \beta'_1) T_t + (\beta_2 + \beta'_2) T_t^2 + (\beta_3 + \beta'_3) T_t^3 + (\beta_4 + \beta'_4) L_t + \varepsilon_t & ; \text{ if } g_1(h, W_d) = 1 \end{cases}$$

[Eq. 5]

Whenever economic activity is in an “active” state, electricity load can be modelled as

$$E_t|(g_1(h, W_d) = 1) = [(\beta_o + \beta'_o) + (\beta_1 + \beta'_1)T_t + (\beta_2 + \beta'_2)T_t^2 + (\beta_3 + \beta'_3)T_t^3 + (\beta_4 + \beta'_4)L_t]. \quad [\text{Eq. 6}]$$

When economic activity is in "rest" state, on the other hand, the model will be

$$E_t|(g_1(h, W_d) = 0) = [\beta_o + \beta_1T_t + \beta_2T_t^2 + \beta_3T_t^3 + \beta_4L_t]. \quad [\text{Eq. 7}]$$

Hence, the proposed model is able to capture differentiated effects of temperature and lighting needs on electricity demand depending on the "state" of economic activity. As can be seen, the proposed model belongs to the general class of switching regression models, where the transition is governed by the smooth function  $g_1(h, W_d)$ . A description about this class of models, and others like the Markov-switching regression models, and the Smooth transition regression models, can be found in [24].

As an alternative model, a HMM model (a good description can be found in [25], Ch. 17) is considered. In this model, the observed variable, electricity load in this analysis, depends on exogenous variables (temperatures and lighting needs), but the relationship between endogenous and exogenous variables responds to two alternative specifications. Whether one or another specification is "the right one" depends on another "hidden" variable that can take as many values as alternative specifications. For the HMM model, "economic activity" is assumed to be the hidden state variable ( $s_t$ ), which at time  $t$  can take on two values (1 = "active" state, 0 = "rest" state). Hence, in the HMM model, electricity load follows the model,

$$E_t = \begin{cases} \phi'_0 + \phi'_1 T_t + \phi'_2 T_t^2 + \phi'_3 T_t^3 + \phi'_4 L_t + \varepsilon_t ; & \text{if } s_t = 1 \\ \phi_0 + \phi_1 T_t + \phi_2 T_t^2 + \phi_3 T_t^3 + \phi_4 L_t + \varepsilon_t ; & \text{if } s_t = 0 \end{cases}$$

[Eq. 8]

where  $s_t$  behaves as a random variable that switches from one state to another. Furthermore,  $s_t$  is assumed to follow a Markov chain with matrix transition probability  $A=[p, 1-p; 1-q, q]$ ; where  $p = P[s_t = 1|s_{t-1} = 1]$  is the probability of remaining in the “active” state between hour  $t$  and hour  $t+1$ , and  $q = P[s_t = 0|s_{t-1} = 0]$  is the probability of remaining in the “rest” state.

Hence, the probability of being in a given state at time  $t$ , depends on the state in the previous period,  $t-1$ , and on the transition probabilities. It is immediate to see the similarities between the HMM model [eq.8] and the LSTR2 model [eq.5]. In the proposed switching regression model with transition function LSTR2 on the other hand, the probability of being in a given state depends only on the hour of the day [0,23]. Two versions of the HMM model are considered, in the first one the probabilities of moving from a state to another are independent of the hour time. In this first HMM model, Given the initial unconditional probabilities of being in a given state at time  $t=0$ ,  $P[s_0 = 1]$ , and  $P[s_0 = 0] = 1 - P[s_0 = 1]$ , the probability of being in state  $s_t$  at time  $t$  is thus given by

$$P_t = A^t P_0, \quad [\text{Eq. 9}]$$

where  $P_t = [P[s_t = 1] \ P[s_t = 0]]'$ , and  $P_0 = [P[s_0 = 1] \ P[s_0 = 0]]'$ .

In our proposed switching regression model with transition function LSTR2 on the other hand, the probability of being in a given state depends only on the hour of the day [0,23]. While this assumption might be considered more restrictive, it is clear that it is more realistic to assume that business activity

responds to a time schedule instead of assuming that business activity at hour  $t$  depends only on business activity at hour  $t-1$ . A second version of the HMM model also considered, assumes that the probability of transition between states depends also on the hour of the day, as in the LSTR2 model. In particular, in this second version of the HMM model the probability,  $p_{ij}$ , of moving from state  $i$  ( $i$ =“rest”, “active”) to state  $j$  ( $j$ = “active”, “rest”) is characterized as a multinomial logit function

$$p_{ij} = \frac{\exp(\alpha^{ij}_0 + \alpha^{ij}_1 h)}{\sum_j \exp(\alpha^{ij}_0 + \alpha^{ij}_1 h)}.$$

As will be detailed in Section 6, it is convenient to impose that economic activity follows the same time schedule throughout the year (excluding holidays and weekends), as assumed in the LSTR2 model. This way one avoids that the yearly temperature cycle (and therefore the daylight cycle) contaminates the estimated state probability in the HMM model. Another advantage of the LSTR2 model is its robustness to the presence of rare events, avoiding identification problems.<sup>9</sup>

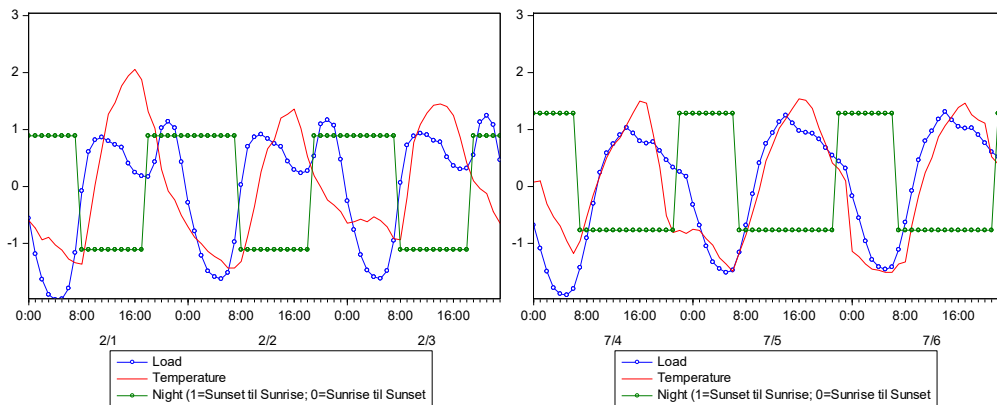
## 5.1. ESTIMATION PROCEDURE AND RESULTS

---

<sup>9</sup> Our model is specific for each type of day (workdays and non-working days) and we only consider national holidays and weekends “non-working days”. However, other regional holidays, mainly in more populated areas in Spain, and e.g. holidays on Tuesdays, which affect economic activity on previous Mondays also have a significant effect on aggregate electricity load. If such events are “rare”, their effect on the estimation of the LSTR2 function is negligible. However, in the HMM model these events would affect identification of the most likely state sequence.

In principle, the model in Equation 4 could be estimated directly by unrestricted nonlinear least squares (NLS). But in practice there are several limitations to adopting this procedure, as also pointed out by [26] (p.213) for the case of Smooth Transition autoregressive model (STAR) estimations. In particular, hours are restricted to the  $[0,23]$  range, and hence parameters  $\tau_1$  and  $\tau_2$  have to satisfy the following constraints  $0 \leq \tau_1 < 23$ ;  $0 \leq \tau_2 \leq 23$ . However, NLS does not guarantee that the estimated values of the time thresholds satisfy such constraints, and hence other estimation procedures are preferred. In addition, NLS usually fails to numerically converge when parameters  $\gamma_d, \tau_1,$  and  $\tau_2$  are estimated jointly. This might be due to the variability throughout the year in the correlation between hourly temperature and the daily economic activity cycle. While in the summer both variables exhibit a near 1:1 correlation, this is not the case in the winter when this correlation is much lower, and variable  $L_t$  takes on a more important role, see Figure 10. Hence, throughout the year, the correlation between temperature and daily economic activity changes, and the smoothness coefficient  $\gamma_d$  and the thresholds  $\tau_1$  and  $\tau_2$  are competing to capture this behavior (wider  $\tau_2 - \tau_1$  ranges compete with lower  $\gamma_d$  values).

Figure 10 Hourly electricity load, hourly temperature and lighting needs. Normalized data. (left, winter: 2/1/2016-2/3/2016, right, summer: 7/4/2016-7/6/2016. workdays only, August excluded)



In order to circumvent the limitations pointed out above, an iterative conditional NLS procedure is proposed. Starting with an initial value for the smoothness coefficient  $\gamma_d^0$ , we compute the optimal threshold parameters,  $\tau_1^0, \tau_2^0$ , that minimize the sum of squared residuals,

$$\tau_1^0, \tau_2^0 = \operatorname{argmin}[\sum_{t=1}^T u_t(\gamma_d^0, \tau_1, \tau_2)^2], \quad [\text{Eq. 10}]$$

where,  $u_t(\gamma_d^0, \tau_1, \tau_2) = (E_t - g_1(h, W_d, \gamma_d^0, \tau_1, \tau_2)g_2(T_t, L_t))$  and,

$$g_1(h, W_d, \gamma_d^0, \tau_1, \tau_2)g_2(T_t, L_t) = [\beta_o + \beta_1 T_t + \beta_2 T_t^2 + \beta_3 T_t^3 + \beta_4 L_t] + [\beta'_o + \beta'_1 T_t + \beta'_2 T_t^2 + \beta'_3 T_t^3 + \beta'_4 L_t]g_1(h', W_d, \gamma_d^0, \tau_1, \tau_2).$$

Optimal thresholds,  $\tau_1^0 = \tau_1^0(\gamma_d^0)$  and  $\tau_2^0 = \tau_2^0(\gamma_d^0)$  are restricted to lie in the intervals,  $\tau_1 \in [4, 11]$ , and  $\tau_2 \in [\tau_1, 23]$ . In each iteration, the parameters  $\beta_i$ , and  $\beta'_i$ , ( $i = 0, 1, \dots, 4$ ) are also estimated. Given the value for  $\gamma_d^0$  and the previously determined thresholds,  $\tau_1^0$  and  $\tau_2^0$ , the conditional sum of squared residuals (SSR) is given by

$$\varphi(\gamma_d^0, \tau_1^0, \tau_2^0) = \sum_{t=1}^T (E_t - g_1(h, W_d, \gamma_d^0, \tau_1^0, \tau_2^0)g_2(T_t, L_t))^2. \quad [\text{Eq. 11}]$$

The iterative procedure aims to minimize this SSR, and the outcome will be the optimal parameter value for  $\gamma_d$  that minimizes the SSR,

$$\gamma_d^* = \operatorname{argmin}[\varphi(\gamma_d^0, \tau_1^0, \tau_2^0)]. \quad [\text{Eq. 12}]$$

Then given  $\gamma_d^*$ , the threshold parameters  $\tau_1^* = \tau_1^*(\gamma_d^*)$  and  $\tau_2^* = \tau_2^*(\gamma_d^*)$  will also be optimal and by construction lie in the range  $[0, 23]$ .

Once  $\gamma_d^*$ ,  $\tau_1^* = \tau_1^*(\gamma_d^*)$ , and  $\tau_2^* = \tau_2^*(\gamma_d^*)$  are determined, the following model is estimated:

$$E_t = g_1(h, W_d, \gamma_d^*, \tau_1^*, \tau_2^*)g_2(T_t, L_t) = [\beta_o + \beta_1 T_t + \beta_2 T_t^2 + \beta_3 T_t^3 + \beta_4 L_t] + [\beta'_o + \beta'_1 T_t + \beta'_2 T_t^2 + \beta'_3 T_t^3 + \beta'_4 L_t]g_1(h', W_d, \gamma_d^*, \tau_1^*, \tau_2^*) + \varepsilon_t.$$

[Eq. 13]

Depending on whether or not the autoregressive term  $\varepsilon_t = \theta_1 \varepsilon_{t-1} + \theta_2 \varepsilon_{t-24} + \vartheta_t$  is included, we estimate two version of this model.,. Note that the autoregressive term tries to capture the approximation errors induced by the linearization of the “true” underlying temperature and lighting effects.

## 6. ESTIMATION RESULTS

The model in Equation 13 is estimated using 9,696 hourly observations for workdays (excluding August) between 1/1/2015 and 12/31/2016. In particular, we use data on hourly electricity load (in logs), temperature (in °C) and a dummy variable  $L_t$  which takes on value 1 if observation  $t$  is after sunset and before sunrise, and 0 otherwise. Results of the estimation are presented in Table 1. Column(1) presents results for the model without and column(2) for the model with autoregressive error terms. In column(3) the estimation results for the HMM model are presented. Column (4) displays the estimation results<sup>10</sup> of an alternative HMM model that includes the hour of the day as an explanatory variable for the state probabilities (“*active*” and “*rest*” states). In all four cases, the models perform relatively well in terms of goodness of fit to the data, keeping in mind the reduced number of parameters required. The mean of the absolute percentage errors (MAPE) ranges from 0.20% to 0.61%. These values, in MWh units instead of logs, represent absolute errors between 2.10% and 10.5% of the mean hourly

---

<sup>10</sup> More details about the estimation of Markov switching models can be found in [26].

electricity load. The HMM, without explanatory variables in the state probabilities, performs worst, with a MAPE of 0.61% or an absolute error of 10.5% if electricity load is measured in MWh. Our proposed LSTR2 model with autoregressive error terms performs best with a MAPE of 0.20% or an absolute error of 2.1% if electricity load is measured in MWh.

Although both versions of the HMM model fit the data well, they have important limitations that make the LSTR2 model more appealing. In particular, one drawback is related to the sign of the estimated coefficient of the  $L_t$  variable in the HMM model. In the two HMM models, the estimated lighting effect is negative, both in the “active” and the “rest” state of economic activity. This result is counterintuitive, since, as Figures 10 or 11 shows, there is a significant increase in electricity load after sunset, with a higher and longer lasting impact if sunset occurs when economic activity is still “active”. This result is due to the fact that in the HMM model, the estimated state probabilities are very sensitive to the “switching on” and “switching off” of lights after sunrise and sunset (see Fig 12 ). However, in the summer (Graph b) of Fig 12), due to the near perfect correlation between hourly electricity load and temperature, the HMM model mistakenly identifies the lighting effect for the “activity” effect. In the simple version of the HMM model this drawback is particularly visible when considering electricity demand in the summer (see Figures 11 and 12). This counterintuitive result may be due to the interaction between the state probabilities and daylight duration, which contaminates the lighting effect when it is estimated simultaneously together with the state probabilities. This problem is not present in the proposed LSTR2 model as the state is estimated by the  $g_1(h', \gamma_d, \tau_1, \tau_2)$  function using a sequential method, which is unique for the full sample.



Figure 11.- Estimated probabilities for economic activity to be in an “active” or “rest” state and data on hourly electricity load (logs MWh) for winter (left graph) and summer (right graph).

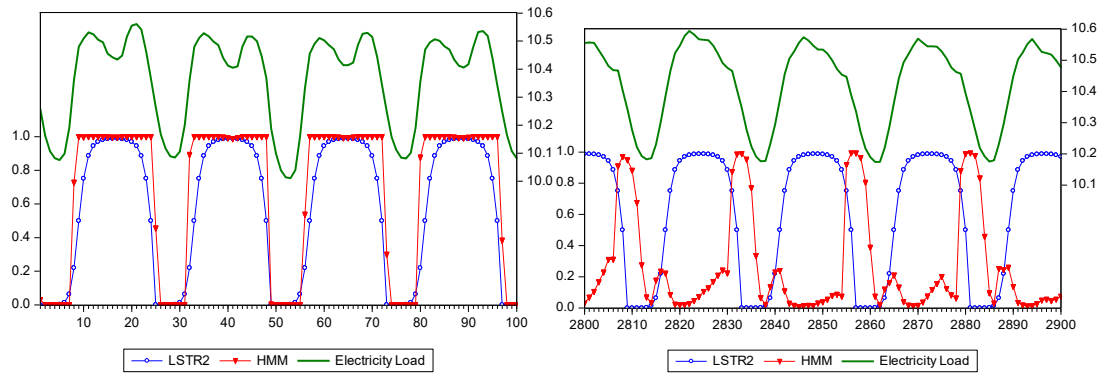
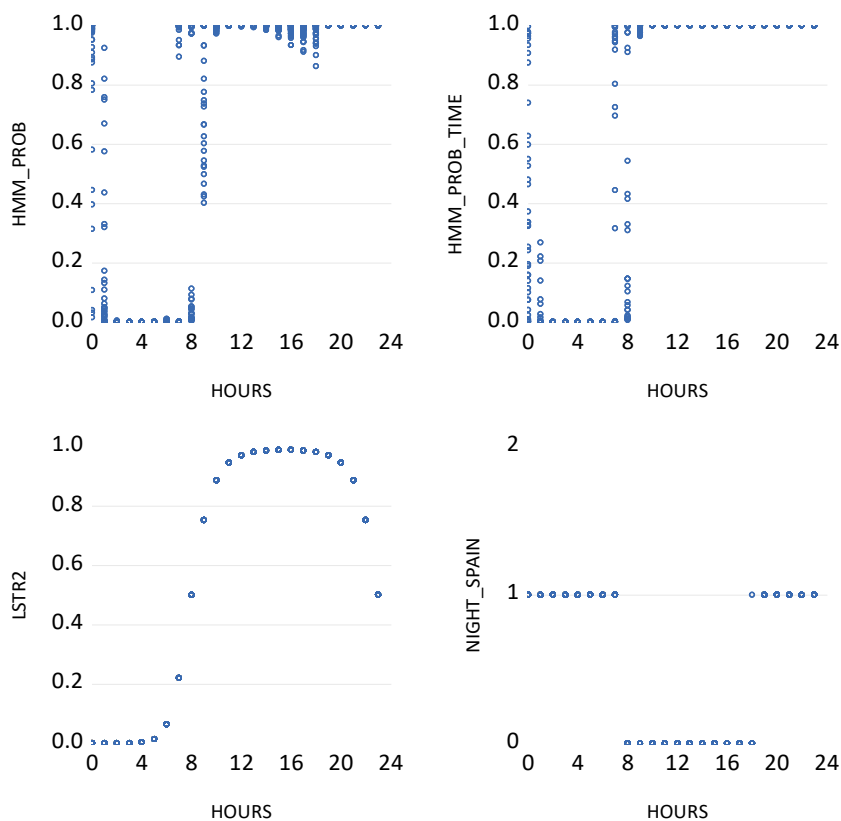
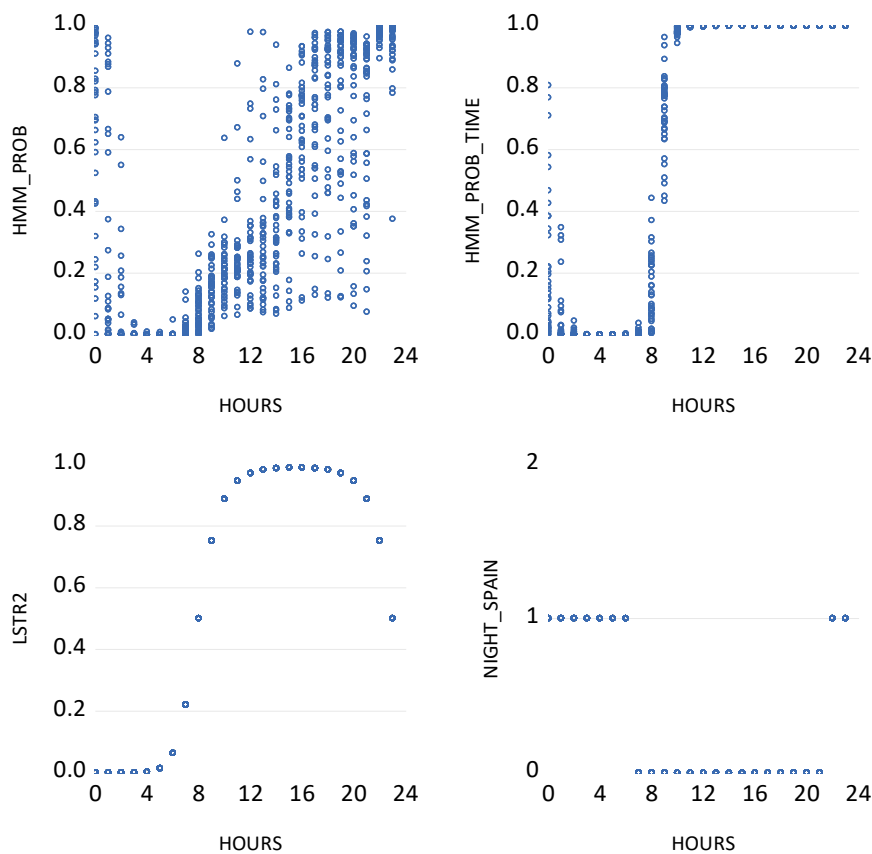


Figure 12.- Estimated probabilities for economic activity to be in an “active” or “rest” state in the HMM model (HMM\_Prob), HMM Model with state probability depending of the hour (HMM\_prob\_time) and LSTR2 model, and  $L_t$  (NIGHT\_SPAIN equal to 1 if the hour is after sunset and before sunrise).

a) Winter (February month)



b) *Summer*



Even more interesting, is the ability of the proposed LSTR2 model to replicate the observed relationship between hourly electricity load and temperature. In Figures 13 and 14, the estimated responses from the LSTR2 model which includes autoregressive error terms are represented.

using the values of the estimated coefficients from Table 1. Figure 13 depicts hourly electricity load data together with the estimated responses, while Figure 14 shows the same variables but differentiated by time of day (hour). As can be seen, the estimated responses allow us to adequately replicate observed differences in the u-shaped relationship between temperatures and electricity load. Only in the case of hours 0 and 1 is the degree of accuracy

not fully satisfactory. This is due to the fact that the function  $g_1(h', \gamma_d, \tau_1, \tau_2)$  is defined in the [0,23] range, with 0 and 23 being the extremes of the function domain, while in the data 0 and 23 are contiguous hours. Given that the estimated values for our parameters are  $\tau_1^* = 8$  and  $\tau_2^* = 23$ , hours 0 and 1 belong to the “rest” state, while 23h, although contiguous to 0h, is a transition hour where function  $g_1(h', \gamma_d, \tau_1, \tau_2)$  takes on value 0.5.

In Figure 13, the estimated model is plotted separately for the two states, given by the extreme values of function  $g_1(h', \gamma_d, \tau_1, \tau_2)$ . According to Equations [5] and [6] - repeated here for convenience - if economic activity is in an “active” state the estimated model is  $E_t|(g_1(h, W_d) = 1) = [(\beta_o + \beta'_o) + (\beta_1 + \beta'_1)T_t + (\beta_2 + \beta'_2)T_t^2 + (\beta_3 + \beta'_3)T_t^3 + (\beta_4 + \beta'_4)L_t]$ .

But in the “rest” state the estimated model is,

$$E_t|(g_1(h, W_d) = 0) = [\beta_o + \beta_1 T_t + \beta_2 T_t^2 + \beta_3 T_t^3 + \beta_4 L_t].$$

These expressions are evaluated using the previously estimated coefficients, and they are plotted against temperatures, taking into account only values of temperatures observed when each state is active.<sup>11</sup> Looking at Figure 13, the asymmetry in the response of electricity demand to temperatures in both states becomes evident. Over the entire range of temperatures, electricity demand in the “active” state is generally higher than in the “rest” state, except when temperatures in the “rest” state rise above 30 °C.

---

<sup>11</sup> The model estimated in each state is only valid for values of the exogenous variables when the given state is active. For example, in the “rest” state, observed temperatures are in the range [-5.4 °C - 31.5° C], while in the “active” state, temperatures lie in the range [-0.7 °C - 40.2° C]. Estimating the two equations over the full range of temperatures produces misleading results.

Table 1 Estimation Results

	Model 1 (LSTR2)			LSTR2 with autoregr..)			HMM Model			HMM Model (State prob. depending of hour time)		
	Coeff	Std. Err.	Sig (95%)	Coeff	Std. Err.	Sig (95%)	Coeff	Std. Err.	Sig (95%)	Coeff	Std. Err.	Sig (95%)
Constant	10.15497	0.005738	**	10.16513	0.002609	**	10.4811	0.005303	**	10.52273	0.005982	**
Temp	-0.004626	0.000966	**	-0.005133	0.000448	**	-0.000279	0.001026		-0.010594	0.001102	**
Temp2	-0.000241	8.61E-05	**	-0.00012	3.96E-05	**	-0.000766	6.16E-05	**	-0.000198	0.0000612	**
Temp3	2.30E-05	2.15E-06	**	1.90E-05	9.88E-07	**	2.14E-05	1.08E-06	**	0.0000133	1.01E-06	**
Lighting	-0.035831	0.004834	**	-0.052008	0.002184	**	-0.02166	0.002185	**	-0.019282	0.002057	**
Constant*f	0.500009	0.010021	**	0.469411	0.004569	**	10.31714	0.004143	**	10.28774	0.004878	**
Temp*f	-0.023715	0.001617	**	-0.020812	0.000743	**	-0.011755	0.000812	**	-0.007891	0.001015	**
Temp2*f	0.000842	0.000111	**	0.000633	5.10E-05	**	0.000623	6.05E-05	**	-0.0000245	0.0000921	
Temp3*f	-2.13E-05	2.45E-06	**	-1.64E-05	1.12E-06	**	-3.41E-06	1.23E-06	**	0.0000171	2.38E-06	**
Lighting*f	0.068026	0.005923	**	0.103111	0.002686	**	-0.187295	0.003008	**	-0.150991	0.003862	**
Err (-1)				0.597187	0.005903	**						
Err (-24)				0.398736	0.005882	**						
S.E. of regression	0.064057			0.028888			0.079408			0.063059		
Sum squared resid	39.68405			8.06134			160.45153			41.20117		
Log likelihood	12891.41			20562.83			11144.95			12283.49		
Akaike info criterion	-2.657057			-4.249552			-2.296193			-2.530629		
PEAM	0.48%			0.20%			0.61%			0.50%		
Theil UI	0.0031			0.0014			0.0063			0.0032		

$$f = g_1(\gamma_d^*, \tau_1^*, \tau_2^*) \quad , \quad \gamma_d^* = -0.0791, \tau_1^* = 8, \tau_2^* = 23$$

Furthermore, the estimated model shows that the sensitivity of demand to low temperatures is significantly larger in the “active” compared to the “rest” state, where very little response is observed. For example, if temperatures decrease from 10 °C to 0 °C, electricity demand in the “active” state increases by 960.5 MWh per 1°C decrease, but by only 26.6 MWh per 1° C decrease in the “rest” state. However, the contrary is true for warm temperatures. If temperatures increase from 21°C to 26°C, electricity demand increases by 323.6 MWh per 1°C in the “active” state, and by 602.9 MWh per 1° C in the “rest” state. However, to correctly interpret these last results it is important to take into account temperature time dynamics in the summer. In particular, between 0h-6h (“rest” state) outdoor temperatures at night are decreasing, while between 10h and 18h (“active” state) temperatures are increasing, and between 18h-23h (“active” state) they are decreasing but only slowly. Hence, the correct way to interpret the elasticity in the “rest state” is a demand decrease by 602.9 MWh per 1° C as temperatures fall from 26°C to 21°C. More importantly, the estimated model highlights that at high temperatures, levels of electricity demand in the “rest” state are similar to those observed in the “active” state.

Figure 13.- Estimated LSTR2 model and electricity load data (MWh logs). Extreme temperature response cases for the “rest” and “active” state of economic activity

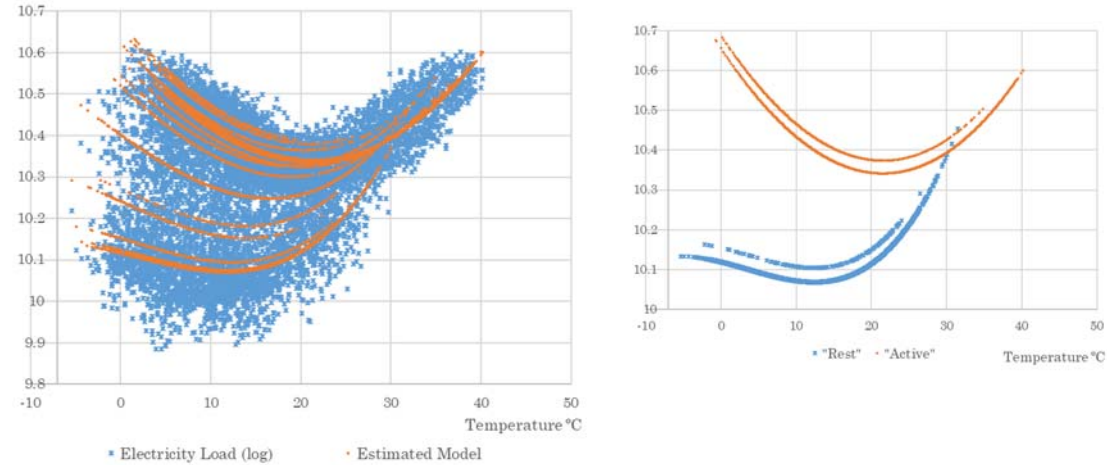
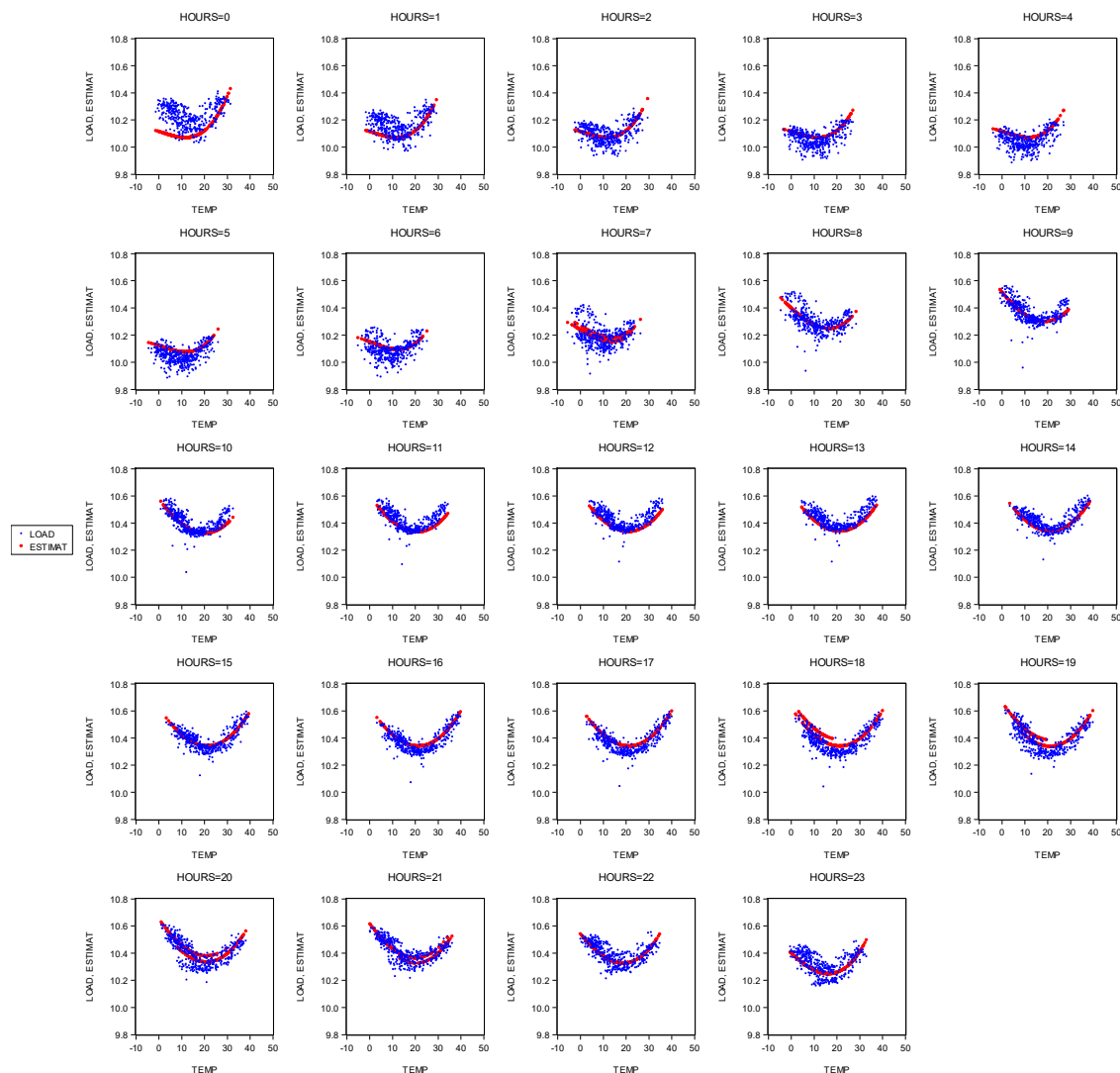


Figure 14.- Estimated time of day temperature response and data on hourly electricity load (logs).



## 7.CONCLUSIONS

Planning, managing and forecasting of electricity demand requires knowing not only the factors that affect it, but exactly when and how these factors impact demand. In particular, if impacts differ by time (hour of day), then

this analysis is not only necessary but mandatory. This paper proposes a model for shortterm electricity demand with differentiated effects by time of day which are determined by variations in intraday economic activity. The relationship between electricity load and economic activity implies that the time properties of the latter directly translate into the former. In particular, the circadian rest-activity cycle and the weekly cycle that affect periods of rest and activity in businesses and working and leisure time of workers is clearly reflected in electricity demand.

The proposed approach allows to differentiate the effects of the circadian rest-activity cycle and the daily and seasonal cycles of temperatures that are caused by the rotation and translation of the earth. Additionally, this movement also affects the insolation cycle, which alters daylight duration. However, this last effect has to be treated separately, given that daylight duration affects different uses of electricity demand (lighting versus heating and cooling) during specific time windows, but also with different intensities according to the degree of economic activity at each hour of the day.

Obviously, the existence of differentiated effects according to uses, and according to time of day, affects the intraday price elasticity of electricity demand. Such differences in elasticity in turn can also affect the effectiveness of differentiated demand response measures such as time-of-day pricing. Peak load in Spain is usually found in the winter on cooler days between 19-20h, due to the combination of heating demand and lighting needs when economic activity is in an “active” state. It is clear that in this situation, electricity demand is price inelastic such that taxing consumption will not have any significant effect on demand in the short run.

The proposed model presents a very satisfactory adjustment to actual data under different statistical measures (Log likelihood, Theil’s U, Sum of squared residuals, AIC criteria). The Logistic Smooth Switching Regression

controlled by a double threshold (LSTR2) without autoregressive error terms attains a mean absolute percentage error of 0.48% (4.95% if electricity load is measured in MWh). When autoregressive error terms are included, the mean absolute percentage error reduces to 0.2% (2.1% if electricity load is measured in MWh).

Based on the observation of the distinct behavior of electricity load when economic activity is in an “active” or in a “rest” state, we also propose a state-of-the-art Hidden Markov Model (HMM) under two different specifications. The best fit to the data is attained when “state” probabilities depend on the hour of the day, as also assumed in our proposed LSTR2 model. Although they both fit the data relatively well, neither version of the HMM model is able to correctly capture how the lighting effect affects electricity load. This limitation of the HMM model seems to be due to the interaction between the yearly cycle of daylight duration and the estimated “state” probabilities, making the LSTR2 model a more promising method for analyzing differentiated effects of temperature and lighting on short-term electricity demand.

## ACKNOWLEDGEMENTS

The authors are grateful to Red Eléctrica de España S.A for their financial support and for providing the data. We also thank Zoe Kuehn for her valuable comments and suggestions. Naturally, the authors remain solely responsible for any errors or omissions.

## REFERENCES



- [1.] Julián Moral-Carcedo and José Vicéns-Otero. Modelling the non-linear response of Spanish electricity demand to temperature variations. *Energy Economics*, Vol. 27, 3, 2005, pp. 477-494.
- [2.] James W. Taylor. Triple seasonal methods for short-term electricity demand forecasting, *European Journal of Operational Research*, Vol. 204, 1, 2010, pp. 139-152.
- [3.] E.J. Palacios-Garcia, A. Moreno-Munoz, I. Santiago, J.M. Flores-Arias, F.J. Bellido-Outeirino, and I.M. Moreno-Garcia. A stochastic modelling and simulation approach to heating and cooling electricity consumption in the residential sector, *Energy*, Vol. 144, 2018, pp. 1080-1091.
- [4.] Anna Marszal-Pomianowska, Per Heiselberg, and Olena Kalyanova Larsen. Household electricity demand profiles – A high-resolution load model to facilitate modelling of energy flexible buildings, *Energy*, Vol 103, 2016, pp. 487-501.
- [5.] Julián Moral-Carcedo, and Julián Pérez-García. Integrating long-term economic scenarios into peak load forecasting: An application to Spain, *Energy*, Vol. 140, 1, 2017, pp. 682-695.
- [6.] European Energy Markets Observatory. 2006 and Winter 2006-2007 Data Set Ninth Edition, November 2007. Colette Lewiner, Ed. CapGemini.

- [7.] REE. Informe del Sistema Eléctrico Español, 2016. REE S.A.  
<http://www.ree.es/es/estadisticas-del-sistema-electrico-espanol/informe-anual/informe-del-sistema-electrico-espanol-2016>
- [8.] Lacir Jorge Soares, and Leonardo Rocha Souza. Forecasting electricity demand using generalized long memory, *International Journal of Forecasting*, Vol 22, 1, 2006, pp. 17-28.
- [9.] Lacir Jorge Soares, and Marcelo C. Medeiros. Modeling and forecasting short-term electricity load: A comparison of methods with an application to Brazilian data, *International Journal of Forecasting*, Vol 24, 4, 2008, pp. 630-644.
- [10.] Rob J. Hyndman and Shu Fan. Density Forecasting for Long-Term Peak Electricity Demand, in *IEEE Transactions on Power Systems*, Vol 25, 2, 2010, pp. 1142-1153.
- [11.] Aleksandra Dedinec, Sonja Filiposka, Aleksandar Dedinec, and Ljupco Kocarev. Deep belief network based electricity load forecasting: An analysis of Macedonian case, *Energy*, Vol. 115, 3, 2016, pp. 1688-1700.
- [12.] Raphael Nedellec, Jairo Cugliari, Yannig Goude, GEFCom2012: Electric load forecasting and backcasting with semi-parametric models, *International Journal of Forecasting*, Vol. 30, 2014, pp. 375–381.

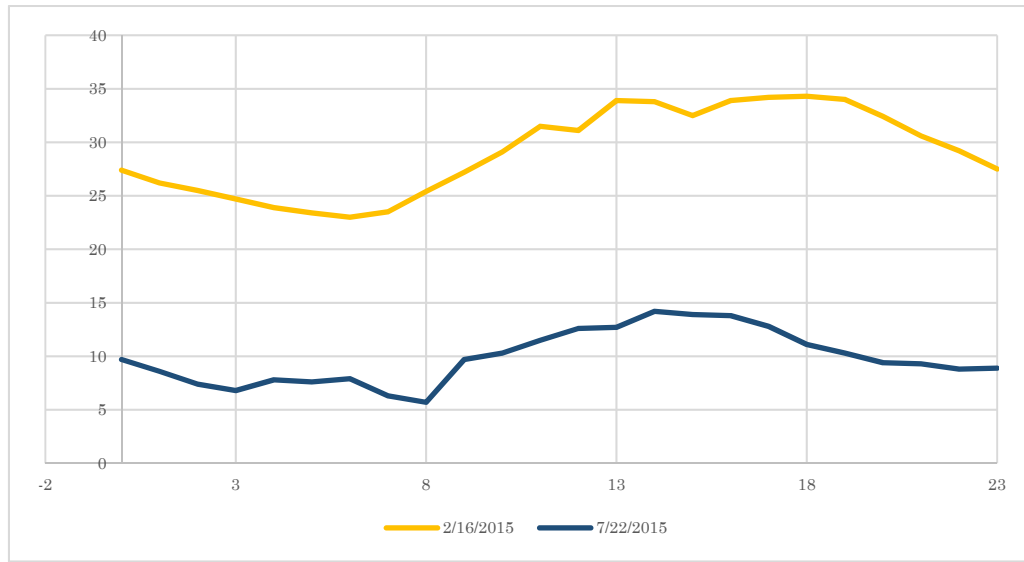
- [13.] Thomas Mestekemper, Göran Kauermann, and Michael S. Smith. A comparison of periodic autoregressive and dynamic factor models in intraday energy demand forecasting, *International Journal of Forecasting*, Vol. 29, 2013, pp. 1-12.
- [14.] Haeran Cho, Yannig Goude, Xavier Brossat, Qiwei Yao. Modelling and forecasting daily electricity load curves: a hybrid approach, *Journal of the American Statistical Association*, Vol. 108, 2013, pp. 7–21.
- [15.] Elena Mocanu, Phuong H. Nguyen, Madeleine Gibescu, Emil Mahler Larsen and Pierre Pinson. Demand forecasting at low aggregation levels using Factored Conditional Restricted Boltzmann Machine, 2016 Power Systems Computation Conference (PSCC), Genoa, 2016, pp. 1-7.
- [16.] Seunghyoung Ryu, Jaekoo Noh and Hongseok Kim. Deep neural network based demand side short term load forecasting, 2016 IEEE International Conference on Smart Grid Communications (SmartGridComm), Sydney, NSW, 2016, pp. 308-313
- [17.] D.J Sailor and A.A Pavlova. Air conditioning market saturation and long-term response of residential cooling energy demand to climate change, *Energy*, Vol. 28, 9, 2003, pp. 941-951.
- [18.] S. Mirasgedis, Y. Sarafidis, E. Georgopoulou, V. Kotroni, K. Lagouvardos, and D.P. Lalas. Modeling framework for estimating

- impacts of climate change on electricity demand at regional level: Case of Greece, *Energy Conversion and Management*, Vol. 48, 5, 2007, pp. 1737-1750.
- [19.] S. Mirasgedis, Y. Sarafidis, E. Georgopoulou, D.P. Lalas, M. Moschovits, F. Karagiannis, and D. Papakonstantinou. Models for mid-term electricity demand forecasting incorporating weather influences, *Energy*, Vol. 31, 2–3, 2006, pp. 208-227.
- [20.] Marie Bessec and Julien Fouquau. The non-linear link between electricity consumption and temperature in Europe: A threshold panel approach, *Energy Economics*, Vol.30, 5, 2008, pp. 2705-2721.
- [21.] Francesco Apadula, Alessandra Bassini, Alberto Elli, and Simone Scapin. Relationships between meteorological variables and monthly electricity demand, *Applied Energy*, Vol. 98, 2012, pp. 346-356.
- [22.] Tianzhen Hong, Wen-Kuei Chang, and Hung-Wen Lin. A fresh look at weather impact on peak electricity demand and energy use of buildings using 30-year actual weather data, *Applied Energy*, Vol. 111, 2013, pp. 333-350.
- [23.] Yaoping Wang, and Jeffrey M. Bielicki. Acclimation and the response of hourly electricity loads to meteorological variables, *Energy*, Vol. 142, 2018, pp. 473-485.

- [24.] Terasvirta, Timo & Tjostheim, Dag & Granger, Clive W. J., 2010. *Modelling Nonlinear Economic Time Series*- Oxford University Press,
- [25.] Kevin P. Murphy. *Machine learning: A probabilistic perspective*. (Ch. 17 Markov and hidden Markov models ). MIT PRESS, 2012
- [26.] Terasvirta, Timo. Specification, Estimation, and Evaluation of Smooth Transition Autoregressive Models. *Journal of the American Statistical Association*, vol. 89, no. 425, 1994, pp. 208–218.
- [27.] Kim, C.J. and Nelson, C. R. *State-Space Models with regime switching*. MIT Press, 1999.

# APPENDIX

Figure A-1 Hourly temperatures in Madrid, Spain for 2015



Source: <https://rp5.ru/>. Non available temperatures are interpolated with a cubic spline.

Table A.1.- Estimation results Hourly Load against temperature in hour I of day t  $E_t^I = f(T_t^I) = a_0^I + a_1^I T_t^I + a_2^I T_t^{I^2} + a_3^I T_t^{I^3}$

	Hour 0		Hour 1		Hour 2		Hour 3		Hour 4		Hour 5		Hour 6	
Variable	Coeff	Std. Err.	Coeff	Std. Err.	Coeff	Std. Err.	Coeff	Std. Err.	Coeff	Std. Err.	Coeff	Std. Err.	Coeff	Std. Err.
Constant	10.32105	0.013475	10.22057	0.011607	10.14524	0.008903	10.09785	0.00702	10.07691	0.006134	10.07797	0.005429	10.1271	0.006419
Temp	-0.013789	0.003692	-0.011376	0.003474	-0.012617	0.002831	-0.011508	0.002371	-0.011976	0.002137	-0.011557	0.00199	-0.013147	0.00238
Temp2	-1.40E-06	0.000286	-1.39E-05	0.000293	0.000345	0.000256	0.000347	0.000232	0.000518	0.00022	0.000453	0.000221	0.000536	0.000277
Temp3	1.75E-05	6.33E-06	1.85E-05	6.99E-06	8.76E-06	6.49E-06	9.32E-06	6.29E-06	4.23E-06	6.21E-06	7.87E-06	6.67E-06	7.57E-06	8.73E-06
R-squared	0.394178		0.363218		0.362412		0.395731		0.377916		0.385756		0.289738	
S.E. of regression	0.061421		0.060126		0.05484		0.049227		0.047932		0.046279		0.057549	
Sum squared resid	1.509039		1.44607		1.202972		0.96931		0.919004		0.856699		1.32477	
AIC criterion	-2.732263		-2.774886		-2.95894		-3.174906		-3.228201		-3.298404		-2.862497	
	Hour 7		Hour 8		Hour 9		Hour 10		Hour 11		Hour 12		Hour 13	
Variable	Coeff	Std. Err.	Coeff	Std. Err.	Coeff	Std. Err.	Coeff	Std. Err.	Coeff	Std. Err.	Coeff	Std. Err.	Coeff	Std. Err.
Constant	10.24409	0.00773	10.39839	0.007751	10.51267	0.011951	10.5975	0.017185	10.64298	0.021404	10.64531	0.024283	10.63374	0.025035
Temp	-0.01485	0.002771	-0.016209	0.002494	-0.017671	0.003326	-0.022457	0.003894	-0.023314	0.004176	-0.02123	0.004318	-0.018915	0.004196
Temp2	0.000531	0.000319	0.000213	0.000246	-2.53E-05	0.000265	0.000172	0.000259	0.000192	0.000245	0.000122	0.000233	6.60E-05	0.000215
Temp3	5.46E-06	9.87E-06	1.23E-05	6.66E-06	1.90E-05	6.05E-06	1.44E-05	5.12E-06	1.23E-05	4.34E-06	1.18E-05	3.84E-06	1.12E-05	3.36E-06
R-squared	0.204182		0.393977		0.543684		0.622207		0.652424		0.66049		0.673203	
S.E. of regression	0.072531		0.060974		0.051025		0.043901		0.040067		0.03824		0.037716	
Sum squared resid	2.104312		1.487132		1.041441		0.770917		0.642158		0.584918		0.569005	
AIC criterion	-2.399747		-2.746886		-3.103131		-3.40391		-3.586657		-3.68002		-3.707601	

Table A.1 (cont.).- Estimation results Hourly Load against temperature in hour I of day t  $E_t^i = f(T_t^i) = a_0^i + a_1^i T_t^i + a_2^i T_t^{i^2} + a_3^i T_t^{i^3}$

	Hour 14		Hour 15		Hour 16		Hour 17		Hour 18		Hour 19		Hour 20	
Variable	Coeff	Std. Err.	Coeff	Std. Err.	Coeff	Std. Err.	Coeff	Std. Err.	Coeff	Std. Err.	Coeff	Std. Err.	Coeff	Std. Err.
Constant	10.59075	0.026322	10.57836	0.025756	10.57872	0.024295	10.58438	0.020792	10.6358	0.018683	10.67298	0.019129	10.66171	0.017976
Temp	-0.013297	0.004257	-0.01569	0.004101	-0.018813	0.003877	-0.023381	0.003453	-0.033348	0.003279	-0.033426	0.003526	-0.028205	0.003554
Temp2	-0.000199	0.00021	-8.81E-05	0.000199	5.86E-05	0.000188	0.000332	0.000171	0.000829	0.000168	0.000713	0.000189	0.000459	0.000202
Temp3	1.45E-05	3.19E-06	1.27E-05	2.97E-06	1.07E-05	2.77E-06	6.50E-06	2.57E-06	-7.51E-07	2.59E-06	1.66E-06	3.00E-06	5.16E-06	3.40E-06
R-squared	0.660519		0.692941		0.724498		0.731942		0.724335		0.684649		0.65872	
S.E. of regression	0.040476		0.040432		0.039894		0.040609		0.043184		0.050576		0.052122	
Sum squared resid	0.655338		0.653885		0.636627		0.659636		0.74595		1.023156		1.086663	
AIC criterion	-3.56634		-3.56856		-3.595306		-3.559803		-3.436833		-3.120844		-3.060624	

	Hour 21		Hour 22		Hour 23	
Variable	Coeff	Std. Err.	Coeff	Std. Err.	Coeff	Std. Err.
Constant	10.61833	0.014416	10.54861	0.01412	10.45016	0.013927
Temp	-0.023017	0.003092	-0.017199	0.003249	-0.016504	0.003513
Temp2	0.000366	0.00019	5.80E-05	0.000213	5.73E-05	0.000251
Temp3	5.17E-06	3.44E-06	1.20E-05	4.06E-06	1.47E-05	5.18E-06
R-squared	0.625033		0.557678		0.470673	
S.E. of regression	0.047226		0.049571		0.05692	
Sum squared resid	0.892105		0.982929		1.295969	
AIC criterion	-3.257908		-3.160954		-2.884477	